DR BO YU (Orcid ID : 0000-0001-8964-7617)
DR YIJING ZHANG (Orcid ID : 0000-0001-9568-9389)
PROFESSOR SHENG TENG (Orcid ID : 0000-0002-5386-6217)

Article type : Original Article

Genome-wide binding analysis reveals that ANAC060 directly represses sugar-induced *ABI5* transcription in Arabidopsis

Bo Yu[1,3†], Yuejun Wang[2,3†], Hua Zhou[1], Ping Li[1], Chunmei Liu[2,3], Sunlu Chen[1,4], Yu Peng[1], Yijing Zhang[2,3*], Sheng Teng[1,3*]

1. Laboratory of Photosynthesis and Environmental Biology, CAS Center for Excellence in Molecular Plant Sciences, Shanghai Institute of Plant Physiology and Ecology, Shanghai Institutes for Biological Sciences, Chinese Academy of Sciences, 300 Fenglin Road, Shanghai 200032, China

2. National Key Laboratory of Plant Molecular Genetics, CAS Center for Excellence in Molecular Plant Sciences, Shanghai Institute of Plant Physiology and Ecology, Shanghai Institutes for Biological Sciences, Chinese Academy of Sciences, 300 Fenglin Road, Shanghai 200032, China

3. University of the Chinese Academy of Sciences, Beijing 100049, China

4. State Key Laboratory of Crop Genetics and Germplasm Enhancement, College of Agriculture, Nanjing Agricultural University, Nanjing 210095, China

† These authors have contributed equally to this work

Correspondence:
Sheng Teng
Laboratory of Photosynthesis and Environmental Biology, CAS Center for Excellence in

Molecular Plant Sciences, Shanghai Institute of Plant Physiology and Ecology, Shanghai Institutes for Biological Sciences, Chinese Academy of Science, 300 Fenglin Road, Shanghai 200032, China
Email: steng@sibs.ac.cn
Tel: +86 21 54924159
Fax: +86 21 54924015

Yijing Zhang
National Key Laboratory of Plant Molecular Genetics, CAS Center for Excellence in Molecular Plant Sciences, Shanghai Institute of Plant Physiology and Ecology, Shanghai Institutes for Biological Sciences, Chinese Academy of Sciences, 300 Fenglin Road, Shanghai 200032, China
Email: zhangyijing@sibs.ac.cn
Tel: +86 21 54924206
Fax: +86 21 54924015

Running head: ANAC060 directly represses *ABI5*

Keywords: *Arabidopsis,* ANAC060, ABI5, transcription factor, sugar signalling.

Summary

Plant sugar status acts as a signal affecting growth and development. The phenomenon by which high-levels of sugars inhibit seedling establishment has been widely used to gain insight into sugar-signaling pathways. Natural allelic variation has been identified at the *ANAC060* locus. In the Columbia ecotype, a short ANAC060 protein without a transmembrane domain (TMD) is produced which is constitutively located to the nucleus causing sugar insensitivity when overexpressed. In this study, we generated a genome-wide DNA binding map of ANAC060 via chromatin immunoprecipitation sequencing (ChIP-seq) using transgenic lines that express a functional ANAC060-GFP fusion protein in an *anac060* background. A total of 3282 genes associated with ANAC060 binding sites were identified. These genes were enriched in biotic and abiotic stress responses, and the G-box binding motif was highly enriched in ANAC060-bound

genomic regions. Expression microarray analysis resulted in the identification of 8350 genes whose activities were altered in the *anac060* mutant and upon sugar treatment. Cluster analysis revealed that *ANAC060* attenuates sugar-regulated gene expression. Direct target genes of ANAC060 included equivalent numbers of genes that were up-regulated or down-regulated by *ANAC060*. The various functions of these target genes indicate that ANAC060 has several functions. Our results demonstrate that ANAC060 directly binds to the promoter of *ABI5* and represses the sugar-induced transcription of *ABI5*. Genetic data indicate that *ABI5* is epistatic to *ANAC060* in both sugar and abscisic Acid (ABA) responses.

Introduction

In plants, photosynthetically produced sugars not only provide energy and the carbon building blocks required for life but also act as signaling molecules. Plants have evolved sophisticated signal transduction systems that link sugar status to growth, development and reproduction (Rolland *et al.*, 2006; Ramon *et al.*, 2008, Smeekens *et al.*, 2010; Wind *et al.*, 2010; Lastdrager *et al.*, 2014; Sheen, 2014, Smeekens and Hellmann, 2014; Li and Sheen, 2016).

Several different sugar molecules and molecular intermediates have been shown to play a role in a variety of signaling pathways and metabolic processes. HXK1 is an intracellular sensor of glucose (Jang *et al.*, 1997; Moore *et al.*, 2003), while RGS1 is an extracellular glucose sensor (Chen and Jones, 2004). The identification of *FINS1*/*FBP* and *ANAC089*-*Cvi*, which are specifically involved in fructose sensitivity, implies the existence of fructose-specific signaling (Cho and Yoo, 2011; Li *et al.*, 2011). SnRK1 has been shown to be a conserved central integrator involved in energy and stress signaling (Baena-Gonzalez *et al.*, 2007). TOR is a central regulator that is highly conserved in eukaryotes (Xiong and Sheen, 2014; Xiong and Sheen, 2015). A glucose-*TOR*-*E2F* pathway has been shown to regulate root meristematic activity (Xiong *et al.*, 2013) and *ROP2*-*TOR*-*E2F* signaling, which is associated with light and auxin responses as well as the activation of the shoot and root apex meristem (Li *et al.*, 2017). Sugar-activating TOR and sugar deprivation-activating SnRK1 regulate the growth and development of plants to facilitate adaptation to various nutrient and energy conditions (Lastdrager *et al.*, 2014; Sheen, 2014; Li and Sheen, 2016). Sugar-signaling pathways also interact with other signaling pathways involved in responses to light, phytohormones, stress, plant defense and nutrients (Rolland *et al.*, 2006; Smeekens *et al.*, 2010; Sheen; 2014).

Several strategies, including glucose insensitivity (*gin*), impaired sucrose induction (*isi*), sugar insensitivity (*sis*) and sucrose uncoupling (*sun*), have been used to screen Arabidopsis sugar-signaling mutants (Smeekens, 2000). To date, more than ten sugar-sensitive mutants have been cloned (Arenas-Huertero *et al.*, 2000; Huijser *et al.*, 2000; Laby *et al.*, 2000; Smeekens, 2000; Rook *et al.*, 2001; Ramon *et al.*, 2008; Funck *et al.*, 2012; Lee *et al.*, 2012; Xiong *et al.*, 2013; Hsu *et al.*, 2014; Huang *et al.*, 2015; Li *et al.*, 2017). Many *gin*, *isi*, *sis* and *sun* mutants are allelic to abscisic acid (ABA)-deficient or ABA-sensitive mutants, highlighting the extensive interaction between sugar signaling and ABA signaling and indicating that ABA plays an important role in glucose signaling. For example, the *gin1/isi4/sis4* mutations are allelic to the ABA biosynthesis gene *ABA2* (Zhou *et al.*, 1998; Laby *et al.*, 2000; Rook *et al.*, 2001; Cheng *et al.*, 2002); the *gin5/isi2/sis3* mutations are allelic to the ABA biosynthesis gene *ABA3* (Arenas-Huertero *et al.*, 2000; Rook *et al.*, 2001); the *sis7* mutation is allelic to the ABA biosynthesis gene *NCED3* (Huang *et al.*, 2008); and the *gin6/isi3/sis5/sun6* mutations are allelic to the ABA-signaling gene *ABI4* (Arenas-Huertero *et al.*, 2000; Huijser *et al.*, 2000; Laby *et al.*, 2000; Rook *et al.*, 2001).

The phenotype of the ABA-signaling mutants *abi2*, *abi3* and *abi5* has also been shown to be insensitive to sugar (Arenas-Huertero *et al.*, 2000; Dekkers *et al.*, 2008; Huang *et al.*, 2008). Mutation in the ABA catabolism gene *CYP707A2* has been shown to induce a glucose-hypersensitive phenotype, whereas *CYP707A2* overexpression lines were only weakly insensitive to glucose (Zhu *et al.*, 2011). Sugar induced the expression of both ABA biosynthesis genes and ABA-signaling genes and repressed ABA catabolism genes (Cheng *et al.*, 2002; Zhu *et al.*, 2011). Overexpression of the glucose sensor *HXK1* in *aba2*/*gin1* and *aba3*/*gin5* backgrounds did not influence the glucose-insensitive phenotype, indicating that ABA signaling acts genetically downstream of HXK1-mediated glucose signaling (Zhou *et al.*, 1998; Arenas-Huertero *et al.*, 2000). Recently, this ABA-mediated sugar signaling has been shown to trigger stomatal closure (Li *et al.*, 2018).

The NAC (NAM, ATAF and CUC) family is a family of plant-specific transcription factors (TFs) whose members have been reported to be primarily involved in plant development and responses to biotic and abiotic stress (Ernst *et al.*, 2004; Nakashima *et al.*, 2012; Puranik *et al.*, 2012). Both *ANAC089* and *ANAC060*, which belong to the *OsNAC8* subgroup of group I NAC TFs, have been found to be involved in sugar signaling. The Cvi allele of *ANAC089* has been shown to be a repressor of fructose sensing and signaling (Li *et al.*, 2011). *ANAC060* has also been shown to play an important role in sugar sensitivity. The short version of ANAC060, which lacks

a transmembrane domain (TMD), is present in approximately 12% of ecotypes, such as Columbia (Col), and induces sugar-insensitive phenotypes (Li *et al.*, 2014). However, the molecular mechanisms underlying how NAC TFs affect sugar sensitivity are still unknown.

Here, we conduct a genome-wide binding analysis of ANAC060 via chromatin immunoprecipitation sequencing (ChIP-seq). Along with a transcriptome analysis of wild-type (WT) plants and *anac060* mutants under glucose treatment, the target genes of ANAC060 were identified to further our understanding of the mechanism underlying how ANAC060 affects sugar-signaling transduction.

Results

ChIP-seq analysis of ANAC060 binding sites under glucose treatment

To investigate the binding sites of ANAC060 at a genome-wide scale *in vivo*, we developed a transgenic line with *CaMV35S*-driven Col-type ANAC060 fused to Green fluorescent protein (GFP) in an *anac060* (Salk_012554C) background (*35S:ANAC060-GFP*/*anac060*). The GFP signal colocalized with 4',6-diamidino-2-phenylindole (DAPI) stain in the nucleus, demonstrating that the ANAC060-GFP fusion protein was localized to the nucleus in the transgenic roots (Figure 1a). The glucose sensitivity of the transgenic lines was similar to that of the WT Col (Figure 1b, c). These results indicated that the ANAC060-GFP fusion protein biologically functioned as an endogenous Col ANAC060 protein.

Seedlings of *35S:ANAC060-GFP*/*anac060* plants used for ChIP-seq analysis were grown on 1/2-strength Murashige and Skoog (MS) medium and supplemented with 6% glucose. The chromatin fragments were prepared via monoclonal anti-GFP antibodies. Anti-GFP ChIP assays were simultaneously performed with the WT as a control. The constructed DNA libraries were then subjected to high-throughput Solexa (Illumina) sequencing. A total of 2860 binding sites on 3282 putative target genes were uniquely assigned (Table S1). Six binding sites were confirmed via ChIP-quantitative real-time PCR (qPCR) (Figure S1).

Genome distribution analysis revealed a strong enrichment of these ANAC060 binding sites in the proximal promoter, which accounted for 70.07% of the total number of binding sites identified (Figure 2a). To investigate the ANAC060 binding profile in the promoter region, the distance between each peak and its nearest gene was calculated. A histogram of these distances at the ±2 kb region around the transcription start sites (TSSs) revealed an enrichment of ANAC060 binding sites in the promoter region, peaking at 200 bp upstream of the TSSs (Figure 2b).

A motif search program (Shao *et al.*, 2012; Wang *et al.*, 2016) was used to analyze the motifs within ±300 bp regions around the ANAC060 binding peaks. The most statistically overrepresented motif was the conserved G-box motif (Figure 2c). Indeed, approximately 34% of the ANAC060 peaks contained one or more typical G-box motifs. The distributional pattern of the G-box motifs around the predicted ANAC060 binding sites (-3000 to +3000 bp) indicated that the motif was overrepresented at the peak in ANAC060 binding sites and decreased to a background level beyond approximately -500 to +500 bp from the peak of ANAC060 binding sites (Figure 2d). An electrophoretic mobility shift assay (EMSA) confirmed that ANAC060 can directly target the G-box motif (Figure 2e). Other enriched motifs included G-box-like, RGCCCA, the TCP family of TFs and some ACGT short sequences.

We also performed ChIP-seq analysis of seedlings grown on 1/2-strength MS medium supplemented with 1% sucrose as a control. Similar to the glucose treatment results, the promoter region was highly enriched with ANAC060 binding sites (Figure S2a), peaking near the TSSs (Figure S2b). Moreover, the G-box motif was also the most statistically overrepresented motif (Figure S2c). A total of 5091 putative target genes were recovered. There were 2464 overlapping genes (75.1% of the genes under glucose treatment and 48.4% of the genes under the control treatment) between these two treatments (Figure S3a). A positive correlation was recorded between the read counts of the common peaks from these two ChIP-seq analyses (Figure S3b).

We then performed a Gene Ontology (GO) analysis of 3282 ANAC060 target genes. ANAC060 tended to bind to genes primarily involved in responses to biotic and abiotic stress, such as chitin, wounding, ABA, cold, and salt; defense responses to fungi; and responses to water deprivation (Figure S4).

The ANAC060 target genes were also compared with the reported target genes of 21 ABA-related TFs. The ANAC060-binding genes highly overlapped those of 16 ABA-related TFs: NF-YB2, GBF3, RD26, HB7, ABF3, HB6, DIV2, GBF2, MYB44, ABF4, NF-YC2, ZAT6, ABF1, HAT22, ANAC032 and HB5 (Song *et al.*, 2016). Additionally, the proportions of overlapping genes ranged from 33.6% to 65.8% of ANAC060 target genes (Table 1).

ANAC060 buffers glucose-triggered transcriptome alterations

To understand the molecular functions of ANAC060 in glucose signaling, we conducted a genome-wide gene expression analysis of both WT and *anac060* under a glucose treatment and a sorbitol osmotic control treatment with three biological replicates. The $\log_2$ values of the signaling

in response to the sorbitol and glucose treatments were plotted for the WT and *anac060* mutants (Figure S5). The degree of variation in expression between the glucose treatment and the sorbitol control treatment was much greater in the *anac060* mutant than in the WT.

The expression levels of a total of 8350 genes were significantly altered between the WT and *anac060* mutant under either the glucose treatment or the sorbitol control treatment or between the glucose treatment and the sorbitol control treatment in either the WT or *anac060* (Tables S2-5). The numbers of up-/down- regulated genes by glucose in the WT and *anac060*, and in *anac060* under glucose treatment and the sorbitol control are shown in Figure 3b, c. The number of glucose-regulated genes in the *anac060* mutant was nearly threefold greater than that in the WT (5955 vs. 2112). ANAC060 affected nearly five times more genes under the glucose treatment than under the sorbitol control treatment (4484 vs. 918).

Cluster analysis divided the differentially expressed genes into 5 groups (Figure 3a). Genes in group 1 were repressed by glucose in the WT and strongly down-regulated in the *anac060* mutant. Genes in group 2 were also repressed by glucose in the WT but up-regulated in the *anac060* mutant. Genes in group 3 were induced by glucose in the *anac060* mutant but not in the WT. Genes in group 4 were induced by glucose in the WT and strongly up-regulated in the *anac060* mutant. Genes in group 5 were also induced by glucose in the WT but down-regulated in the *anac060* mutant.

There were 3496 (41.86%) genes in group 1 and group 2 that were effectively down-regulated by glucose in the WT. Among those genes, approximately 73.9% that were clustered in group 1 were more strongly down-regulated by glucose in the *anac060* mutant than in the WT. Representative sugar-repressed marker genes, such as *CAB*, *PC* and *RBCS*, were found in group 1. A total of 4854 (58.13%) genes in group 3, group 4 and group 5 were effectively up-regulated by glucose in the WT. Approximately 65.9% of these genes, which were clustered in group 3 or group 4, exhibited stronger glucose up-regulation in the *anac060* mutant than in the WT. Marker genes up-regulated by sugar, such as *ABI3*, *ABI4*, *ABI5* and *APL3*, were in these two groups (Figure 3a). These results indicated that the *anac060* mutant exhibited more pronounced variation in both gene number and gene expression levels between the glucose treatment and the sorbitol control treatment than the WT, implying that ANAC060 globally attenuates glucose-regulated gene expression.

To investigate the roles of ANAC060 in glucose sensing and signaling more comprehensively, two Venn diagrams were constructed based on genes that were

up-/down-regulated by glucose and in the *anac060* mutant (Figure 3b, c). There were a total of 926 glucose-induced and ANAC060-repressed genes (Figure 3b, Table S6). GO enrichment analysis indicated that these genes were primarily enriched in the seed dormancy process, lipid storage, response to ABA, seed germination, response to ethylene, response to water deprivation, DNA-dependent DNA replication, the terpenoid biosynthesis process, response to freezing and the gibberellin biosynthesis process (Figure 3d).

There were 1806 glucose-repressed and ANAC060-activated genes (Figure 3c, Table S7). GO enrichment analysis revealed that these genes were primarily enriched in the chloroplast thylakoid membrane, chloroplast thylakoid, photosynthesis, light reactions, thylakoids, response to nitrate, nitrate transport, plastid organization, photosystem II assembly and rRNA processing (Figure 3e).

Functions of genes activated and repressed by ANAC060

Five hundred genes were common between 3282 ANAC060-binding genes and 4484 differentially expressed genes between the WT and *anac060* mutant under glucose treatment. These 500 genes were considered to be direct target genes of ANAC060. Among these 500 genes, the expression of 215 was up-regulated in the *anac060* mutant (Figure 4a, Table S8), whereas the expression of 285 was down-regulated in the *anac060* mutant (Figure 4a, Table S9).

Among 215 ANAC060-repressed genes, the expression of 113 genes was also up-regulated by glucose, most of which probably contributed to the glucose-hypersensitive phenotype of the *anac060* mutant (Table S10). GO analysis revealed that these 113 genes were enriched in the response to ABA, the response to water deprivation, the seed dormancy process, the ABA-activated signaling pathway, protein binding and lipid storage (Figure 4b). Two of these GO terms were related to ABA signaling. Twenty-three genes, including *ABI5*, were involved in these GO terms (Figure 4d).

Among 285 ANAC060-activated genes, the expression of 199 genes was also down-regulated by glucose, which was probably responsible for the glucose-hypersensitive phenotype of the *anac060* mutant (Table S11). There were 30 enriched GO terms detected from these 199 genes. The top ten enriched GO terms were associated with the response to nitrate, nitrate transport, divalent metal ion transport, cellular cation homeostasis, chloroplast thylakoids, chloroplast thylakoid membranes, the response to cyclopentenone, photosynthesis, the light reactions, thylakoids and indole-3-acetic amino acid synthetase activity (Figure 4c). Interestingly, among the

30 enriched GO terms, eight were related to chloroplasts and photosynthesis. Twenty-seven genes, including *RBSC*, *CAB* and *PC*, were involved in these GO terms (Figure 4e).

ANAC060 directly repressed *ABI5* expression

Functional ABA signaling is essential for sugar sensitivity. Therefore, the ANAC060 target genes involved in the response to ABA and ABA-activated signaling pathways were further investigated. Among these genes, *ABI5*, one of the central components of the ABA-signaling pathway, was specifically examined in detail. Based on our ChIP-seq data, we found that the ANAC060 binding site can enrich the *ABI5* promoter, indicating that ANAC060 can bind to the *ABI5* promoter (Figure 5a). The binding of ANAC060 to the *ABI5* promoter *in vivo* was confirmed by ChIP-qPCR (Figure 5b). There were four G-box motifs in the promoter region of *ABI5* (-192 to -197 bp, -203 to -208 bp, -249 to -254 bp and -725 to-730 bp from the TSS) (Figure 5c). Two tightly linked G-box motifs were located within the region of -190 to -206 bp upstream of the TSS.

The EMSA revealed that the ANAC060-glutathione S-transferase (GST) fusion protein can bind to the fragment (from -172 to -227 bp upstream of the TSS) that contains these two G-box motifs *in vitro*, whereas the GST protein cannot bind to this fragment (Figure 5d). Mutation in either of the G-box motifs abolished this binding activity (Figure 5d). qPCR-based detection indicated that glucose induction of *ABI5* expression dramatically increased in the *anac060* mutant compared with the WT. The introduction of *35S:ANAC060-GFP* in the *anac060* mutant reduced the activity of glucose inducing *ABI5* expression (Figure 5e). These results confirmed the findings from microarray experiments and revealed that ANAC060 represses *ABI5* expression under glucose treatment. The repression effect of ANAC060 on *ABI5* promoter activity was further confirmed via a luciferase transient expression assay in *Nicotiana benthamiana* leaves (Figure 5f). These results indicated that ANAC060 directly binds to the *ABI5* promoter and represses *ABI5* expression.

The *anac060/abi5* double mutant was insensitive to glucose and ABA

anac060/abi5 double mutants were generated to investigate the effects of *ABI5* repression by ANAC060 on sugar and ABA sensitivity. *abi5* mutants were insensitive to glucose, whereas the *anac060* mutant exhibited a glucose super-sensitive phenotype (Figure 6a, b; Figure S6a, b). *anac060/abi5* double mutants displayed a glucose-insensitive phenotype similar to that of *abi5* mutants (Figure 6a, b; Figure S6a, b). Similarly, ABA-induced *ABI5* expression was also increased in *anac060* mutants (Figure S7), and *anac060/abi5* double mutants were also insensitive to ABA, as were *abi5* mutants (Figure 6c, d; Figure S6c, d). These results indicated that the repression of *ABI5* by ANAC060 contributed to sugar and ABA insensitivity.

Discussion

NAC TFs are specific to plants. Identification of the binding sites and binding motifs of NAC TFs is essential for determining their functions. Previously, NAC protein binding sites and motifs have been identified from the promoter sequence of a single NAC target gene (Xie *et al.*, 2000; Fujita *et al.*, 2004; Tran *et al.*, 2004b). The binding sites and binding motifs of three NAC TFs, RD26, ANAC032 and ANAC102, have been recently identified via ChIP-seq (Song *et al.*, 2016), and those of 62 NAC TFs have also been identified via a recently developed high-throughput technology, DNA affinity purification sequencing (DAP-seq) (O'Malley *et al.*, 2016). These results indicated that the binding sites and binding motifs of different NAC TFs can differ drastically (O'Malley *et al.*, 2016; Song *et al.*, 2016). However, the binding sites of ANAC060 and its close homologs ANAC040 and ANAC089, which belong to the OsNAC8 subgroup of group I NAC TFs, were not included in these 65 NAC TFs. The identification of ANAC060 binding sites at a genome-wide scale in this study will contribute to a more complete understanding of the function of the NAC TF family members.

Enrichment of G-box binding motifs was strong within ANAC060 binding sites, implying that the TF function of ANAC060 is mediated by binding G-box elements in the promoters of its target genes. Previous studies have shown that the ANAC protein binds to the CACG (a part of G-box) motif (Tran *et al.*, 2004a; Olsen *et al.*, 2005). *In vitro* DAP-seq identified CGTG (another part of G-box) as the ANAC protein binding motif (O'Malley *et al.*, 2016). Interestingly, *in vivo* ChIP-seq has shown that RD26 (ANAC072) binding sites are enriched in G-box (CACGTG) (Song *et al.*, 2016), yet *in vitro* binding assays have found that RD26 can bind to the E-box (CATGTG, a specialized G-box) and that this binding activity is enhanced by the interaction between RD26 with BES1 (Ye *et al.*, 2017). Future work is needed to further explore the complexity of the ANAC060 regulation network. Recently, the G-box was recognized via ChIP-seq as a binding motif of TFs involved in ABA signaling (Song *et al.*, 2016) and light signaling (Lee *et al.*, 2007; Zhang *et al.*, 2013; Pfeiffer *et al.*, 2014). Fruitful avenues of future work include examining the roles of TFs that bind to the same motif in different biological processes as well as the roles of the flanking bases.

The naturally varied, constitutively functional version of ANAC060 has been previously shown to attenuate ABA signaling and render sugar insensitivity (Li *et al.*, 2014). In this study, we did not find any glucose sensors, such as TOR or SnRK1, in the list of ANAC060 target genes

(Table S8, Table S9), implying that ANAC060 primarily functions downstream of the sugar-signaling pathway. ChIP-seq analysis indicated that ANAC060 tends to bind genes involved in the stress response, and its suite of target genes overlaps extensively with genes targeted by ABA-related TFs, implying that ANAC060 is involved in stress and ABA responses. Transcriptome analysis revealed that, between the WT and *anac060* mutant, there were more genes with altered expression under the glucose treatment than under the osmotic control treatment. These results indicated that *ANAC060* plays an important role in the sugar response. Furthermore, the expression of sugar-regulated genes was more severely altered in the *anac060* mutant than in the WT, indicating that ANAC060 acts as a buffer in the glucose-signaling pathway at the scale of the entire genome and transcriptome. The identification of chloroplast thylakoid and photosynthesis genes (Figure 3e) in the glucose-treated *anac060* mutant reflected the effect of ANAC060 on downstream transcriptomic responses to glucose. Further exploration of the effect of ANAC060 on the immediate transcriptomic response to glucose using treated materials over short time windows would be a most interesting direction of future research.

Previous work has confirmed the transcriptional activation function of ANAC060 (Li *et al.*, 2014). In this study, 500 target genes of ANAC060 were identified via a combination of ChIP-seq and microarray analysis. Among these genes, the expression of 285 (57%) was up-regulated by ANAC060, and the expression of 215 (43%) genes was down-regulated by ANAC060. The repression function of ANAC060 on *ABI5* was also confirmed (Figure 5). These results indicated that, similar to ABI4 (Wind *et al.*, 2013), ANAC060 is a dual-function TF that acts not only as a transcriptional activator but also as a transcriptional repressor.

We have previously detected natural variation in the sub-cellular localization of ANAC060 among Arabidopsis accessions (Li *et al.*, 2014). The present study indicated that nucleus-localized ANAC060 tends to bind to genes involved in responses to diverse sources of biotic and abiotic stress. Recently, ANAC060 has been identified as a candidate gene of the QTL for seed dormancy and seedling emergence timing (Footitt *et al.*, 2019). The direct activation of *ABI5* by nucleus-localized ANAC060 under glucose treatment could also explain the putative function of ANAC060 in seed dormancy and seedling emergence timing.

As a core component of the ABA-signaling pathway and an integrator of ABA signaling and other phytohormone signaling, ABI5 plays an important role in seed germination and seedling establishment. ABI5 is regulated by multiple TFs, epigenetic factors and protein regulators (Skubacz *et al.*, 2016). The transcription of *ABI5* is positively regulated by *MYB96*, *DOG1*, *ABI5*

itself and *HY5* (Xu *et al.*, 2014; Skubacz *et al.*, 2016). *ABI5* is also negatively regulated by *SAG*, *WRKY60*, *WRKY40*, *WRKY18*, *MYB7*, *PED3*, *RAV1* and *BBX21* (Skubacz *et al.*, 2016). In this study, ANAC060 was defined as a direct negative regulator of *ABI5*. How these transcription factors coordinately regulate ABI5 and the relationship between these transcription factors are intriguing. ABI5 has been shown to bind to its own promoter throughout three G-box motifs to activate itself (Xu *et al.*, 2014). Interestingly, our results indicated that ANAC060 binds to the same G-box region on the *ABI5* promoter to repress *ABI5* expression. How ANAC060 physically and functionally competes with ABI5 as well as whether ANAC060 interferes with the transcriptional activity of ABI5 or other transcription factors requires further study. These studies promise to contribute to a more complete understanding of the regulatory network of *ABI5* expression.

ABI4 and *ABI5* are essential for sugar sensitivity and act synergistically (Reeves *et al.*, 2011). Positive self-feedback regulation has been documented for these two genes (Bossi *et al.*, 2009; Skubacz *et al.*, 2016). ABI4 has been shown to play an important positive role in sugar-induced *ABI5* expression (Arroyo *et al.*, 2003). Furthermore, ABI4 has been shown to bind the CE-1-like motif in the promoter of *ABI5* and directly activate the expression of *ABI5* (Bossi *et al.*, 2009). ABI5 is also essential for sugar-induced *ABI4* expression (Arroyo *et al.*, 2003). These results indicated that a positive regulatory network exists between *ABI4* and *ABI5*. Previously, we have found that ABI4 directly activated *ANAC060* (Li *et al.*, 2014). However, ANAC060 does not directly regulate *ABI4* (Figure S8) but *ABI5*. The results of the present study suggest that a negative regulatory mechanism exists between *ABI4* and *ABI5* via *ANAC060*, illustrating the complexity of the ABI4 and ABI5 regulatory network.

Experimental procedures

Plant materials

Arabidopsis thaliana accession Col was used as the WT. The mutant *anac060* (Salk_012554C) (Li *et al.*, 2014) and the *abi5-7* mutation that causes a premature stop codon at W^{75} in the *ABI5* gene (Nambara *et al.*, 2002) were described previously. *35S:ANAC060-GFP/anac060* transgenic lines were generated as described here. PCR for ANAC060 cDNA was performed using the primers presented in Table S12. The PCR products were digested with EcoRI and SalI and subsequently cloned into 35S:GFP-pCAMBIA1300. The

35S:ANAC060-GFP-pCAMBIA1300 vector was then introduced into Agrobacterium, which was subsequently transformed into *anac060* (Salk_012554C) plants using the floral dip method (Zhang *et al.*, 2006).

ChIP-seq and ChIP-qPCR

Two grams of 10-d-old whole seedlings of *35S:ANAC060-GFP/anac060* transgenic plants were used for ChIP assays as described previously (He *et al.*, 2012, Li *et al.*, 2014). WT (Col) plants grown under the same conditions were used as the control. Polyclonal anti-GFP antibodies (Abcam, ab290) were used to immunoprecipitate the chromatin complexes. Sequencing libraries were constructed according to Illumina's instructions. The end-repaired DNA fragments were ligated to an adaptor. Afterward, DNA fragments of 200-300 bp were recovered by gel purification and then amplified by PCR. The amplified DNA products were validated by a Bioanalyzer 2000 (Agilent, Germany) and sequenced with an Illumina HiSeq 2500 system. A total of 23,557,726 reads were obtained. The precipitated DNA from the ChIP assay was also used for qPCR with primers for different binding sites (Table S12). The fold enrichment was calculated as the ratio between the precipitated DNA and the input and normalized to that of the *Ubiquitin* promoter, whose value was arbitrarily fixed at 1.0.

Bioinformatics analysis of ChIP-seq data

The raw sequencing reads were cleaned by removing bases that had low quality scores (<20) and irregular GC content, removing sequencing adaptors and filtering out short reads by Trimmomatic (Bolger *et al.*, 2014). As a result, 3 to 10 million reads with a mapping quality (MAPQ) score > 20 were obtained for further analyses. The cleaned reads were mapped to the *A. thaliana* genome (TAIR10) using BWA 0.7.5a-r405 (Li and Durbin, 2009) with the default settings, and uniquely mapped reads with MAPQ > 20 were collected for further analysis.

MACS 1.4 (Zhang *et al.*, 2008) was used for peak calling of the ChIP-seq datasets, with a no-antibody ChIP control comprising Col-0 seedlings under parameters --shiftsize=100 and --pvalue=1e-10. The target gene of each peak was defined as the gene closest to a given peak within 500 bp centered on the TSS.

Motif search and classification

To detect TF-binding motifs enriched within ANAC060 binding peak regions, we

downloaded 924 position weight matrixes (PWMs) from four major plant motif databases, namely, JASPAR (228 motifs) (Mathelier *et al.*, 2014), AthaMap (183 motifs) (Hehl and Bulow, 2014), AGRIS (91 motifs) (Yilmaz *et al.*, 2011), and PLACE (422 motifs) (Higo *et al.*, 1999). We then performed a motif scan within a 1000 bp window centered on the peak center (Shao *et al.*, 2012, Wang *et al.*, 2016). For each motif M, the raw motif matching score at each peak P was calculated as $\max_{S \subseteq P} \left[log \frac{P(S|M)}{P(S|B)} \right]$, in which S is a sequence fragment of the same length as the motif and B is the background frequency of four types of nucleotides (A, C, G, and T) estimated from the genome. The enrichment of motif M in a peak list was defined as the ratio of the motif occurrence in the peak list in comparison to its occurrence in random genomic regions. Fisher's exact test (Fisher, 1945) was used to calculate the enrichment *P* value.

Microarray and data analyses

An Agilent Arabidopsis 3.0 Oligo Microarray kit, which contains nearly 40,000 features representing 28,500 genes, was used to investigate the transcriptomes of the WT and *anac060* mutants under both glucose and sorbitol control treatments with three biological replicates. Total RNA was isolated from seedlings using an RNeasy Plant Mini Kit (Qiagen, 74903). cDNA and cRNA synthesis, cRNA labeling and fragmentation, chip hybridization and washing were performed according to the One-Color Microarray-Based Gene Expression Analysis instructions from Agilent Technologies. Gene chip array hybridization signals were scanned with an Agilent scanner (G2505c) in accordance with the Expression Analysis Technical Manual.

Raw data in txt format were preprocessed using limma (Ritchie *et al.*, 2015), and then differentially expressed genes were detected based on 4 comparisons. Two criteria were used to define the differentially expressed genes: $|\log_2 \text{fold change}| > 1$ and adjusted *P* value < 0.05.

The gene annotation files and GO terms were downloaded from The Arabidopsis Information Resource (TAIR) homepage (http://www.arabidopsis.org). Enrichment analysis of functional terms and clustering of related terms were performed as described previously (Wang *et al.*, 2015).

K-means clustering was applied to partition gene sets and comparisons into different clusters according to expression profiles by an open source clustering software Cluster 3.0 (de Hoon *et al.*, 2004), with parameters 1000 number of runs and similarity metric calculating by Euclidean distance.

Quantitative real-time PCR qPCR

Total RNA was extracted from seedlings using an RNeasy Plant Mini Kit (Qiagen, 74903). One microgram of RNA was used for cDNA synthesis with SuperScript™ III First-Strand Synthesis SuperMix (Invitrogen, 11752-050). Real-time PCR was performed using FastStart Universal SYBR Green Master (ROX) (Roche, 04913914001) with a Roche Light Cycler 96 SW 1.0 Real-Time PCR system sequence detector. The gene expression levels were normalized to those of *PP2A*. The primers used in qPCR are listed in Table S12.

Expression and purification of fusion proteins and EMSAs

The *ANAC060* cDNA was cloned into a pGEX4T-1 (GE Healthcare) vector, which was subsequently transfected into BL21 cells (Transgene). When the bacterium culture reached an OD_{600} of 1.0, expression of the GST-ANAC060 fusion protein was induced with 1 mM isopropyl-1-thio-D-galactopyranoside at 16°C for 24 h. The fusion proteins within the collected bacterium cultures were then purified via Glutathione Sepharose 4 fast flow resin (GE Healthcare).

The EMSAs were performed by a LightShift® Chemiluminescent EMSA Kit (Thermo, 20148), with slight modifications. Approximately 50 bp-long DNA probes (Table S12) were synthesized, and their 5' ends were labeled with Cy5 or 5-carboxyfluorescein (FAM) (Invitrogen). One microliter of probes and 1 μg of purified proteins per reaction were incubated with binding buffer at room temperature for 20 minutes in accordance with the manufacturer's instructions. The samples were then loaded onto 4% agarose gels, which were run in Tris/borate/EDTA (TBE) buffer on ice for 1 h. The labeled probes were imaged by a Fujifilm FLA 9000 plus DAGE.

Promoter activity assays

The promoter activity was assayed in *N. benthamiana* plants as described previously (Hellens *et al.*, 2005). The 2 kb *ABI5* promoter was amplified (Table S12) and cloned to construct *pGreenII ABI5-LUC* (firefly luciferase) vectors, which served as a reporter. The effectors were *pGreenII 35S-ANAC060* vectors with full-length *ANAC060* cDNA driven by the cauliflower mosaic virus 35S promoter. The vectors were transfected into Agrobacterium GV3101 cells. The Agrobacterium cells were subsequently cultured overnight, after which they were resuspended in infiltration media (10 mM MgCl2, 0.5 μM acetosyringone) to an OD_{600} of 1.0. The reporters and effectors were mixed together at a ratio of 1:9, after which the mixture was infiltrated into young *N. benthamiana* leaves. At 3 days after infiltration, the promoter activity was assayed using a

Dual-Luciferase® Reporter Assay System (Promega, E1910) according to the manufacturer's instructions. *pGreenII 62-SK* was used as a control, and the values were arbitrarily fixed at 1.0.

Accession numbers

ChIP-seq and RNA-seq data reported in this study have been deposited at the National Center for Biotechnology Information. (Gene Expression Omnibus accession no. GSE123123, GSE123169 and GSE123170).

Acknowledgments

The authors thank all the lab members for their inspirational discussions. The authors are grateful for the help from Prof. Lin Xu with respect to the ChIP experiments and Dr. Xiaoshu Gao with respect to the confocal observations. This work was supported by the National Key R&D Program of China (2016YFD0100700), the Ministry of Agriculture of China for Transgenic Research (2016ZX08009003-004) and the National Natural Science Foundation (U19A2025, 31870229 and 31370284).

AUTHOR CONTRIBUTIONS

The scientific concept and the experimental design were developed by BY and ST. BY and HZ, PL, YP performed all experiments. BY, YW, CL, YZ and ST analyzed the data. BY and ST wrote the manuscript. All contributing authors approved the manuscript and agreed to be accountable for all aspects of the work.

CONFLICT OF INTEREST

The authors declare no conflict of interests.

Supporting Information

Figure S1 ChIP-qPCR assays verified six ANAC060 direct binding targets *in vivo*.

Figure S2 Genome-wide identification of ANAC060 binding sites under control medium (1% sucrose).

Figure S3 Comparison of the ChIP-seq analyses under control medium and glucose treatment.

Figure S4 GO enrichment of ANAC060-binding genes under glucose treatment.

Figure S5 Expression variation between sorbitol and glucose treatments in the WT and *anac060* mutant.

Figure S6 Genetic interaction between *ANAC060* and *ABI5* in sugar and ABA sensitivity.

Figure S7 Expression of *ABI5* in Col and *anac060* under ABA treatment.

Figure S8 ANAC060 indirectly activates *ABI4*.

Table S1 List of ANAC060_binding_genes.

Table S2 List of glucose regulated genes in the WT.

Table S3 List of glucose regulated genes in *anac060* mutant.

Table S4 List of altered expression genes in *anac060* mutant under sorbitol treatment.

Table S5 List of altered expression genes in *anac060* mutant under glucose treatment.

Table S6 List of glucose upregulated and ANAC060 downregulated_genes.

Table S7 List of glucose downregulated and ANAC060 upregulated _genes.

Table S8 List of ANAC060 directly repressed genes.

Table S9 List of ANAC060 directly activated genes.

Table S10 List of ANAC060 directly repressed and glucose upregulated genes.

Table S11 List of ANAC060 directly activated and glucose downregulated genes.

Table S12 Sequences of the primers and probes.

Reference

Arenas-Huertero, F., Arroyo, A., Zhou, L., Sheen, J. and Leon, P. (2000) Analysis of Arabidopsis glucose insensitive mutants, gin5 and gin6, reveals a central role of the plant hormone ABA in the regulation of plant vegetative development by sugar. *Gene Dev*, **14**, 2085-2096.

Arroyo, A., Bossi, F., Finkelstein, R.R. and Leon, P. (2003) Three genes that affect sugar sensing (Abscisic Acid Insensitive 4, Abscisic Acid Insensitive 5, and Constitutive Triple Response 1) are differentially regulated by glucose in arabidopsis. *Plant physiology*, **133**, 231-242.

Baena-Gonzalez, E., Rolland, F., Thevelein, J.M. and Sheen, J. (2007) A central integrator of transcription networks in plant stress and energy signalling. *Nature*, **448**, 938-942.

Bolger, A.M., Lohse, M. and Usadel, B. (2014) Trimmomatic: a flexible trimmer for Illumina sequence data. *Bioinformatics*, **30**, 2114-2120.

Bossi, F., Cordoba, E., Dupre, P., Mendoza, M.S., Roman, C.S. and Leon, P. (2009) The

Arabidopsis ABA-INSENSITIVE (ABI) 4 factor acts as a central transcription activator of the expression of its own gene, and for the induction of ABI5 and SBE2.2 genes during sugar signaling. *Plant Journal*, **59**, 359-374.

Chen, J.G. and Jones, A.M. (2004) AtRGS1 function in Arabidopsis thaliana. *Methods in enzymology*, **389**, 338-350.

Cheng, W.H., Endo, A., Zhou, L., Penney, J., Chen, H.C., Arroyo, A., Leon, P., Nambara, E., Asami, T., Seo, M., Koshiba, T. and Sheen, J. (2002) A unique short-chain dehydrogenase/reductase in Arabidopsis glucose signaling and abscisic acid biosynthesis and functions. *The Plant cell*, **14**, 2723-2743.

Cho, Y.H. and Yoo, S.D. (2011) Signaling role of fructose mediated by FINS1/FBP in Arabidopsis thaliana. *PLoS genetics*, **7**, e1001263.

de Hoon, M.J., Imoto, S., Nolan, J. and Miyano, S. (2004) Open source clustering software. *Bioinformatics*, **20**, 1453-1454.

Dekkers, B.J.W., Schuurmans, J.A.M.J. and Smeekens, S.C.M. (2008) Interaction between sugar and abscisic acid signalling during early seedling development in Arabidopsis. *Plant molecular biology*, **67**, 151-167.

Ernst, H.A., Olsen, A.N., Skriver, K., Larsen, S. and Lo Leggio, L. (2004) Structure of the conserved domain of ANAC, a member of the NAC family of transcription factors. *Embo Rep*, **5**, 297-303.

Fisher, R.A. (1945) A New Test for 2x2 Tables. *Nature*, **156**, 388-388.

Footitt, S., Walley, P.G., Lynn, J.R., Hambidge, A.J., Penfield, S. and Finch-Savage, W.E. (2019) Trait analysis reveals DOG1 determines initial depth of seed dormancy, but not changes during dormancy cycling that result in seedling emergence timing. *New Phytol*.

Fujita, M., Fujita, Y., Maruyama, K., Seki, M., Hiratsu, K., Ohme-Takagi, M., Tran, L.S.P., Yamaguchi-Shinozaki, K. and Shinozaki, K. (2004) A dehydration-induced NAC protein, RD26, is involved in a novel ABA-dependent stress-signaling pathway. *Plant Journal*, **39**, 863-876.

Funck, D., Clauss, K., Frommer, W.B. and Hellmann, H.A. (2012) The Arabidopsis CstF64-like RSR1/ESP1 protein participates in glucose signaling and flowering time control. *Front Plant Sci*, **3**.

He, C.S., Chen, X.F., Huang, H. and Xu, L. (2012) Reprogramming of H3K27me3 Is Critical for Acquisition of Pluripotency from Cultured Arabidopsis Tissues. *PLoS genetics*, **8**.

Hehl, R. and Bulow, L. (2014) AthaMap web tools for the analysis of transcriptional and posttranscriptional regulation of gene expression in Arabidopsis thaliana. *Methods Mol Biol*, **1158**, 139-156.

Hellens, R.P., Allan, A.C., Friel, E.N., Bolitho, K., Grafton, K., Templeton, M.D., Karunairetnam, S., Gleave, A.P. and Laing, W.A. (2005) Transient expression vectors for functional genomics, quantification of promoter activity and RNA silencing in plants. *Plant Methods*, **1**.

Higo, K., Ugawa, Y., Iwamoto, M. and Korenaga, T. (1999) Plant cis-acting regulatory DNA elements (PLACE) database: 1999. *Nucleic Acids Res*, **27**, 297-300.

Hsu, Y.F., Chen, Y.C., Hsiao, Y.C., Wang, B.J., Lin, S.Y., Cheng, W.H., Jauh, G.Y., Harada, J.J. and Wang, C.S. (2014) AtRH57, a DEAD-box RNA helicase, is involved in feedback inhibition of glucose-mediated abscisic acid accumulation during seedling development and additively affects pre-ribosomal RNA processing with high glucose. *Plant Journal*, **77**, 119-135.

Huang, L.M., Lai, C.P., Chen, L.F.O., Chan, M.T. and Shaw, J.F. (2015) Arabidopsis SFAR4 is a novel GDSL-type esterase involved in fatty acid degradation and glucose tolerance. *Bot Stud*, **56**.

Huang, Y.D., Li, C.Y., Biddle, K.D. and Gibson, S.I. (2008) Identification, cloning and characterization of sis7 and sis10 sugar-insensitive mutants of Arabidopsis. *BMC plant biology*, **8**.

Huijser, C., Kortstee, A., Pego, J., Weisbeek, P., Wisman, E. and Smeekens, S. (2000) The Arabidopsis SUCROSE UNCOUPLED-6 gene is identical to ABSCISIC ACID INSENSITIVE-4: involvement of abscisic acid in sugar responses. *Plant Journal*, **23**, 577-585.

Jang, J.C., Leon, P., Zhou, L. and Sheen, J. (1997) Hexokinase as a sugar sensor in higher plants. *The Plant cell*, **9**, 5-19.

Laby, R.J., Kincaid, M.S., Kim, D. and Gibson, S.I. (2000) The Arabidopsis sugar-insensitive mutants sis4 and sis5 are defective in abscisic acid synthesis and response. *The Plant journal : for cell and molecular biology*, **23**, 587-596.

Lastdrager, J., Hanson, J. and Smeekens, S. (2014) Sugar signals and the control of plant growth and development. *Journal of experimental botany*, **65**, 799-807.

Lee, J., He, K., Stolc, V., Lee, H., Figueroa, P., Gao, Y., Tongprasit, W., Zhao, H., Lee, I. and

Deng, X.W. (2007) Analysis of transcription factor HY5 genomic binding sites revealed its hierarchical role in light regulation of development. *The Plant cell*, **19**, 731-749.

Lee, S.A., Yoon, E.K., Heo, J.O., Lee, M.H., Hwang, I., Cheong, H., Lee, W.S., Hwang, Y.S. and Lim, J. (2012) Analysis of Arabidopsis glucose insensitive growth Mutants Reveals the Involvement of the Plastidial Copper Transporter PAA1 in Glucose-Induced Intracellular Signaling. *Plant physiology*, **159**, 1001-1012.

Li, H. and Durbin, R. (2009) Fast and accurate short read alignment with Burrows-Wheeler transform. *Bioinformatics*, **25**, 1754-1760.

Li, L. and Sheen, J. (2016) Dynamic and diverse sugar signaling. *Current opinion in plant biology*, **33**, 116-125.

Li, P., Wind, J.J., Shi, X.L., Zhang, H.L., Hanson, J., Smeekens, S.C. and Teng, S. (2011) Fructose sensitivity is suppressed in Arabidopsis by the transcription factor ANAC089 lacking the membrane-bound domain. *Proceedings of the National Academy of Sciences of the United States of America*, **108**, 3436-3441.

Li, P., Zhou, H., Shi, X., Yu, B., Zhou, Y., Chen, S., Wang, Y., Peng, Y., Meyer, R.C., Smeekens, S.C. and Teng, S. (2014) The ABI4-induced Arabidopsis ANAC060 transcription factor attenuates ABA signaling and renders seedlings sugar insensitive when present in the nucleus. *PLoS genetics*, **10**, e1004213.

Li, X., Cai, W., Liu, Y., Li, H., Fu, L., Liu, Z., Xu, L., Liu, H., Xu, T. and Xiong, Y. (2017) Differential TOR activation and cell proliferation in Arabidopsis root and shoot apexes. *Proceedings of the National Academy of Sciences of the United States of America*.

Li, Y., Xu, S.S., Wang, Z.W., He, L.C., Xu, K. and Wang, G.X. (2018) Glucose triggers stomatal closure mediated by basal signaling through HXK1 and PYR/RCAR receptors in Arabidopsis. *Journal of experimental botany*, **69**, 1471-1484.

Mathelier, A., Zhao, X., Zhang, A.W., Parcy, F., Worsley-Hunt, R., Arenillas, D.J., Buchman, S., Chen, C.Y., Chou, A., Ienasescu, H., Lim, J., Shyr, C., Tan, G., Zhou, M., Lenhard, B., Sandelin, A. and Wasserman, W.W. (2014) JASPAR 2014: an extensively expanded and updated open-access database of transcription factor binding profiles. *Nucleic Acids Res*, **42**, D142-147.

Moore, B., Zhou, L., Rolland, F., Hall, Q., Cheng, W.H., Liu, Y.X., Hwang, I., Jones, T. and Sheen, J. (2003) Role of the Arabidopsis glucose sensor HXK1 in nutrient, light, and hormonal signaling. *Science*, **300**, 332-336.

Nakashima, K., Takasaki, H., Mizoi, J., Shinozaki, K. and Yamaguchi-Shinozaki, K. (2012) NAC transcription factors in plant abiotic stress responses. *Bba-Gene Regul Mech*, **1819**, 97-103.

Nambara, E., Suzuki, M., Abrams, S., McCarty, D.R., Kamiya, Y. and McCourt, P. (2002) A screen for genes that function in abscisic acid signaling in Arabidopsis thaliana. *Genetics*, **161**, 1247-1255.

O'Malley, R.C., Huang, S.S.C., Song, L., Lewsey, M.G., Bartlett, A., Nery, J.R., Galli, M., Gallavotti, A. and Ecker, J.R. (2016) Cistrome and Epicistrome Features Shape the Regulatory DNA Landscape (vol 165, pg 1280, 2016). *Cell*, **166**, 1598-1598.

Olsen, A.N., Ernst, H.A., Lo Leggio, L. and Skriver, K. (2005) NAC transcription factors: structurally distinct, functionally diverse. *Trends in plant science*, **10**, 79-87.

Pfeiffer, A., Shi, H., Tepperman, J.M., Zhang, Y. and Quail, P.H. (2014) Combinatorial complexity in a transcriptionally centered signaling hub in Arabidopsis. *Molecular plant*, **7**, 1598-1618.

Puranik, S., Sahu, P.P., Srivastava, P.S. and Prasad, M. (2012) NAC proteins: regulation and role in stress tolerance. *Trends in plant science*, **17**, 369-381.

Ramon, M., Rolland, F. and Sheen, J. (2008) Sugar sensing and signaling. *The Arabidopsis book / American Society of Plant Biologists*, **6**, e0117.

Reeves, W.M., Lynch, T.J., Mobin, R. and Finkelstein, R.R. (2011) Direct targets of the transcription factors ABA-Insensitive(ABI)4 and ABI5 reveal synergistic action by ABI4 and several bZIP ABA response factors. *Plant molecular biology*, **75**, 347-363.

Ritchie, M.E., Phipson, B., Wu, D., Hu, Y., Law, C.W., Shi, W. and Smyth, G.K. (2015) limma powers differential expression analyses for RNA-sequencing and microarray studies. *Nucleic Acids Res*, **43**, e47.

Rolland, F., Baena-Gonzalez, E. and Sheen, J. (2006) Sugar sensing and signaling in plants: conserved and novel mechanisms. *Annual review of plant biology*, **57**, 675-709.

Rook, F., Corke, F., Card, R., Munz, G., Smith, C. and Bevan, M.W. (2001) Impaired sucrose-induction mutants reveal the modulation of sugar-induced starch biosynthetic gene expression by abscisic acid signalling. *The Plant journal : for cell and molecular biology*, **26**, 421-433.

Shao, Z., Zhang, Y., Yuan, G.C., Orkin, S.H. and Waxman, D.J. (2012) MAnorm: a robust model for quantitative comparison of ChIP-Seq data sets. *Genome Biol*, **13**, R16.

Sheen, J. (2014) Master Regulators in Plant Glucose Signaling Networks. **57**, 67-79.

Skubacz, A., Daszkowska-Golec, A. and Szarejko, L. (2016) The Role and Regulation of ABI5 (ABA-Insensitive 5) in Plant Development, Abiotic Stress Responses and Phytohormone Crosstalk. *Front Plant Sci*, **7**.

Smeekens, S. (2000) Sugar-induced signal transduction in plants. *Annual review of plant physiology and plant molecular biology*, **51**, 49-81.

Smeekens, S. and Hellmann, H.A. (2014) Sugar sensing and signaling in plants. *Front Plant Sci*, **5**.

Smeekens, S., Ma, J.K., Hanson, J. and Rolland, F. (2010) Sugar signals and molecular networks controlling plant growth. *Current opinion in plant biology*, **13**, 274-279.

Song, L., Huang, S.S.C., Wise, A., Castanon, R., Nery, J.R., Chen, H.M., Watanabe, M., Thomas, J., Bar-Joseph, Z. and Ecker, J.R. (2016) A transcription factor hierarchy defines an environmental stress response network. *Science*, **354**.

Tran, L.S., Nakashima, K., Sakuma, Y., Simpson, S.D., Fujita, Y., Maruyama, K., Fujita, M., Seki, M., Shinozaki, K. and Yamaguchi-Shinozaki, K. (2004a) Isolation and functional analysis of Arabidopsis stress-inducible NAC transcription factors that bind to a drought-responsive cis-element in the early responsive to dehydration stress 1 promoter. *The Plant cell*, **16**, 2481-2498.

Tran, L.S.P., Nakashima, K., Sakuma, Y., Simpson, S.D., Fujita, Y., Maruyama, K., Fujita, M., Seki, M., Shinozaki, K. and Yamaguchi-Shinozaki, K. (2004b) Isolation and functional analysis of Arabidopsis stress-inducible NAC transcription factors that bind to a drought-responsive cis-element in the early responsive to dehydration stress 1 promoter. *The Plant cell*, **16**, 2481-2498.

Wang, H., Liu, C., Cheng, J., Liu, J., Zhang, L., He, C., Shen, W.H., Jin, H., Xu, L. and Zhang, Y. (2016) Arabidopsis Flower and Embryo Developmental Genes are Repressed in Seedlings by Different Combinations of Polycomb Group Proteins in Association with Distinct Sets of Cis-regulatory Elements. *PLoS genetics*, **12**, e1005771.

Wang, J., Qi, M., Liu, J. and Zhang, Y. (2015) CARMO: a comprehensive annotation platform for functional exploration of rice multi-omics data. *Plant J*, **83**, 359-374.

Wind, J., Smeekens, S. and Hanson, J. (2010) Sucrose: metabolite and signaling molecule. *Phytochemistry*, **71**, 1610-1614.

Wind, J.J., Peviani, A., Snel, B., Hanson, J. and Smeekens, S.C. (2013) ABI4: versatile

activator and repressor. *Trends in plant science*, **18**, 125-132.

Xie, Q., Frugis, G., Colgan, D. and Chua, N.H. (2000) Arabidopsis NAC1 transduces auxin signal downstream of TIR1 to promote lateral root development. *Gene Dev*, **14**, 3024-3036.

Xiong, Y., McCormack, M., Li, L., Hall, Q., Xiang, C. and Sheen, J. (2013) Glucose-TOR signalling reprograms the transcriptome and activates meristems. *Nature*, **496**, 181-186.

Xiong, Y. and Sheen, J. (2014) The role of target of rapamycin signaling networks in plant growth and metabolism. *Plant physiology*, **164**, 499-512.

Xiong, Y. and Sheen, J. (2015) Novel links in the plant TOR kinase signaling network. *Current opinion in plant biology*, **28**, 83-91.

Xu, D.Q., Li, J.G., Gangappa, S.N., Hettiarachchi, C., Lin, F., Andersson, M.X., Jiang, Y., Deng, X.W. and Holm, M. (2014) Convergence of Light and ABA Signaling on the ABI5 Promoter. *PLoS genetics*, **10**.

Ye, H.X., Liu, S.Z., Tang, B.Y., Chen, J.N., Xie, Z.L., Nolan, T.M., Jiang, H., Guo, H.Q., Lin, H.Y., Li, L., Wang, Y.Q., Tong, H.N., Zhang, M.C., Chu, C.C., Li, Z.H., Aluru, M., Aluru, S., Schnable, P.S. and Yin, Y.H. (2017) RD26 mediates crosstalk between drought and brassinosteroid signalling pathways. *Nature communications*, **8**.

Yilmaz, A., Mejia-Guerra, M.K., Kurz, K., Liang, X., Welch, L. and Grotewold, E. (2011) AGRIS: the Arabidopsis Gene Regulatory Information Server, an update. *Nucleic Acids Res*, **39**, D1118-1122.

Zhang, X.R., Henriques, R., Lin, S.S., Niu, Q.W. and Chua, N.H. (2006) Agrobacterium-mediated transformation of Arabidopsis thaliana using the floral dip method. *Nat Protoc*, **1**, 641-646.

Zhang, Y., Liu, T., Meyer, C.A., Eeckhoute, J., Johnson, D.S., Bernstein, B.E., Nusbaum, C., Myers, R.M., Brown, M., Li, W. and Liu, X.S. (2008) Model-based analysis of ChIP-Seq (MACS). *Genome Biol*, **9**, R137.

Zhang, Y., Mayba, O., Pfeiffer, A., Shi, H., Tepperman, J.M., Speed, T.P. and Quail, P.H. (2013) A quartet of PIF bHLH factors provides a transcriptionally centered signaling hub that regulates seedling morphogenesis through differential expression-patterning of shared target genes in Arabidopsis. *PLoS genetics*, **9**, e1003244.

Zhou, L., Jang, J.C., Jones, T.L. and Sheen, J. (1998) Glucose and ethylene signal transduction crosstalk revealed by an Arabidopsis glucose-insensitive mutant. *Proceedings of the*

National Academy of Sciences of the United States of America, **95**, 10294-10299.

Zhu, G., Liu, Y., Ye, N., Liu, R. and Zhang, J. (2011) Involvement of the abscisic acid catabolic gene CYP707A2 in the glucose-induced delay in seed germination and post-germination growth of Arabidopsis. *Physiol Plant*, **143**, 375-384.

Figure Legends

Figure 1 Transgenic line with *CaMV35S*-driven biologically functional *ANAC060-GFP* in the *anac060* background. (a) The ANAC060-GFP fusion protein was located in the nucleus of *35S:ANAC060-GFP/anac060* transgenic plants. The nuclear positions were marked by DAPI staining. The merged image comprises merged images of the Dic, GFP channel and DAPI channel. (b), (c) Glucose-sensitive phenotypes (b) and rates of greening seedlings (c). Seedlings were grown on a 1/2-strength MS agar plate that contained either 6% glucose or 6% sorbitol for 9 days at 22°C under constant light at 3 days after stratification. The error bars mean SEs (n=3). Sor: sorbitol. Glc: glucose.

Figure 2 Genome-wide identification of ANAC060 binding sites under 6% glucose treatment. (a) Genomic distribution of ANAC060 binding peaks. Promoter class defined as 2 kb upstream of the gene TSS. (b) Distribution of ANAC060 binding peaks relative to gene structure (-2000 bp from the TSS to +2000 bp downstream of the 3' end). (c) Motif analysis of ANAC060 peaks revealed a G-box as the top enriched motif. (d) Distribution of the G-box around the ANAC060 binding peaks. (e) ANAC060 directly bound to a DNA fragment that contains a G-box (CACGTG). DNA fragments that contain a G-box (CACGTG) or mutant fragments (CACGTG mutated to AAAAAA) labeled by Cy5. Unlabeled WT fragments (100- and 200-fold) were used as a cold competitive probe.

Figure 3 *ANAC060* attenuated glucose signaling. (a) K-means clustering of differentially expressed genes. The number and percentage of the genes in each group are marked under the group number. Sor: sorbitol. Glc: glucose. vs: comparison. (b) Venn diagram showing the overlap of genes upregulated by glucose treatment in the *anac060* mutant. The P values of overlapping between *anac060*_Glc_vs_Col_Glc up (Blue cycle) and *anac060*_Glc_vs_*anac060*_Sor up (Green cycle) was less than 7.040e-154. (c) Venn diagram showing the overlap of genes downregulated by glucose treatment in the *anac060* mutant. The P values of overlapping between *anac060*_Glc_vs_Col_Glc down (Blue cycle) and *anac060*_Glc_vs_*anac060*_Sor down (Green cycle) was 0. (d) GO enrichment analysis of genes upregulated in the *anac060* mutant and by glucose treatment. (e) GO enrichment analysis of genes downregulated in the *anac060* mutant and by glucose treatment.

Figure 4 Identification of ANAC060 direct target genes. (a) Venn diagram representing the direct target genes of ANAC060 under glucose treatment. (b) GO enrichment analysis of ANAC060-directly repressed and glucose-upregulated genes. (c) GO enrichment analysis of ANAC060-directly activated and glucose-downregulated genes. (d) Heat map of the microarray data of ANAC060-directly repressed ABA-related genes in response to glucose. (e) Heat map of the microarray data of ANAC060-directly activated photosynthesis-related genes in response to glucose.

Figure 5 ANAC060 directly repressed *ABI5* expression. (a) Integrative genomics viewer (IGV) screenshots showing visualization of the ANAC060 binding profile of the *ABI5* promoter. Immunoprecipitated Col DNA fragments were used as a control. (b) ChIP-qPCR assays verified the direct binding of ANAC060 to the *ABI5* promote*r in vivo*. Ten-day-old *35S:ANAC060-GFP/anac060* seedlings were used for ChIP assays, after which the DNA fragments were immunoprecipitated by anti-GFP antibodies. The fold enrichment was normalized to that of the *Tubulin* promoter, whose values were arbitrarily fixed at 1.0. The error bars mean SEs (n=3). * P<0.01 (Student's t test). (c) The position of G-box motifs within the *ABI5* promoter and the sequences of the probes used for EMSAs. Four G-box (CACGTG) motifs were identified in the promoter of *ABI5*. A 56 bp DNA fragment that contained two G-box motifs representing the binding peak in Figure 5(a) was used for the EMSAs. The two G-box sequences within the probe were mutated individually or simultaneously (CACGTG to AAAAAA). (d) ANAC060 binding to *ABI5* promoter via G-box. One microgram of purified GST-ANAC060 or GST protein was incubated with the 5' FAM-labeled WT or mutated DNA fragments that had the sequence shown in Figure 5(c). Unlabeled WT DNA fragments (100- and 200-fold) were used as cold competitors. (e) Expression of *ABI5* in Col, *anac060* and *35S:ANAC060-GFP/anac060* under glucose treatment. Seedlings were grown on 1/2-strength MS agar plates that contained 6% glucose or 6% sorbitol for 7 days. The error bars mean SEs (n=3). *PP2A* was used as reference. (f) Transient expression assays of luciferase activity in *N. benthamiana* leaves revealed that ANAC060 repressed the activity of the *ABI5* promoter. A 2 kb *ABI5* promoter fused to a firefly luciferase coding sequence served as reporter. *CaMV35S* fused to *ANAC060* served as an effector, and empty *pGreenII 62-SK* vectors served as a control. *35S-Renilla LUC* was used as an internal control. The error bars mean SEs (n=3). * P<0.01 (Student's t test).

Figure 6 Genetic interaction between *ANAC060* and *ABI5* with respect to sugar and ABA sensitivity. (a), (b) Glucose-sensitive phenotypes (a) and greening seedling rates (b) of Col, *anac060*, *abi5-7* and the *anac060*/*abi5-7* double mutant. Seeds were plated on 1/2-strength MS agar that contained 6% glucose or 6% sorbitol for 9 days at 22°C under constant light at 3 days after stratification. The error bars mean SEs (n=3). (c), (d). ABA sensitivity (c) and greening seedling rate (d) of Col, *anac060*, *abi5-7* and the *anac060*/*abi5-7* double mutant. Seeds were plated on 1/2-strength MS agar that was supplemented with or without 0.5 μM ABA for 7 days at 22°C under constant light at 3 days after stratification. The error bars mean SEs (n=3)

Table 1 Overlap between the targets of ANAC060 and ABA-related TFs

ABA-related TFs	Number of TF targets	Number of ANAC060 targets	Number of overlaps	Overlap ratio (%)	P-value
NF-YB2	10,159	3,282	2,159	65.8	0
GBF3	8,191	3,282	1,848	56.3	0
RD26	7,579	3,282	1,701	51.8	0
HB7	8,092	3,282	1,699	51.8	1E-283
ABF3	7,458	3,282	1,672	50.9	1.1E-316
HB6	6,826	3,282	1,657	50.5	0
DIV2	6,586	3,282	1,492	45.5	1.1E-275
GBF2	5,726	3,282	1,477	45.0	0
MYB44	6,210	3,282	1,466	44.7	3.7E-291
ABF4	5,619	3,282	1,390	42.4	2.5E-295
NF-YC2	4,805	3,282	1,374	41.9	0
ZAT6	5,563	3,282	1,321	40.2	1.1E-256
ABF1	5,025	3,282	1,259	38.4	4.9E-266
HAT22	5,027	3,282	1,199	36.5	1E-228
ANAC032	4,656	3,282	1,180	36.0	2.4E-250
HB5	4,881	3,282	1,104	33.6	4E-186

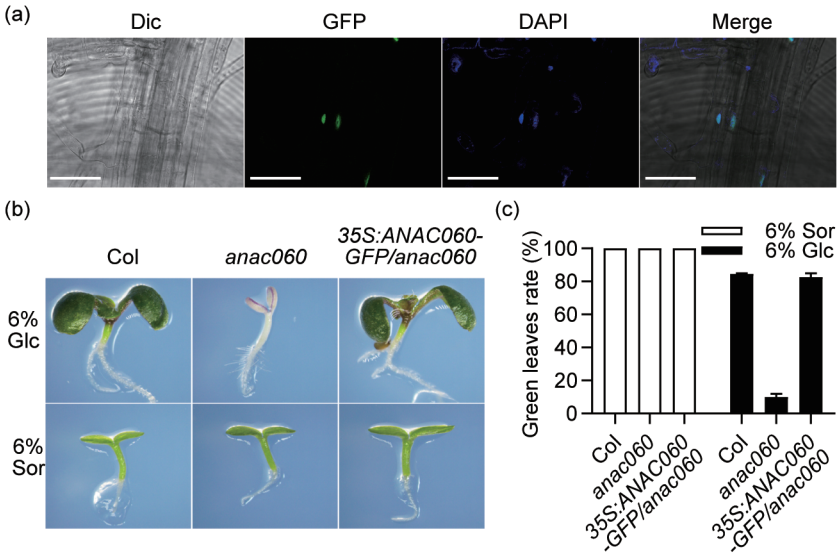

tpj_14777_f1.tif

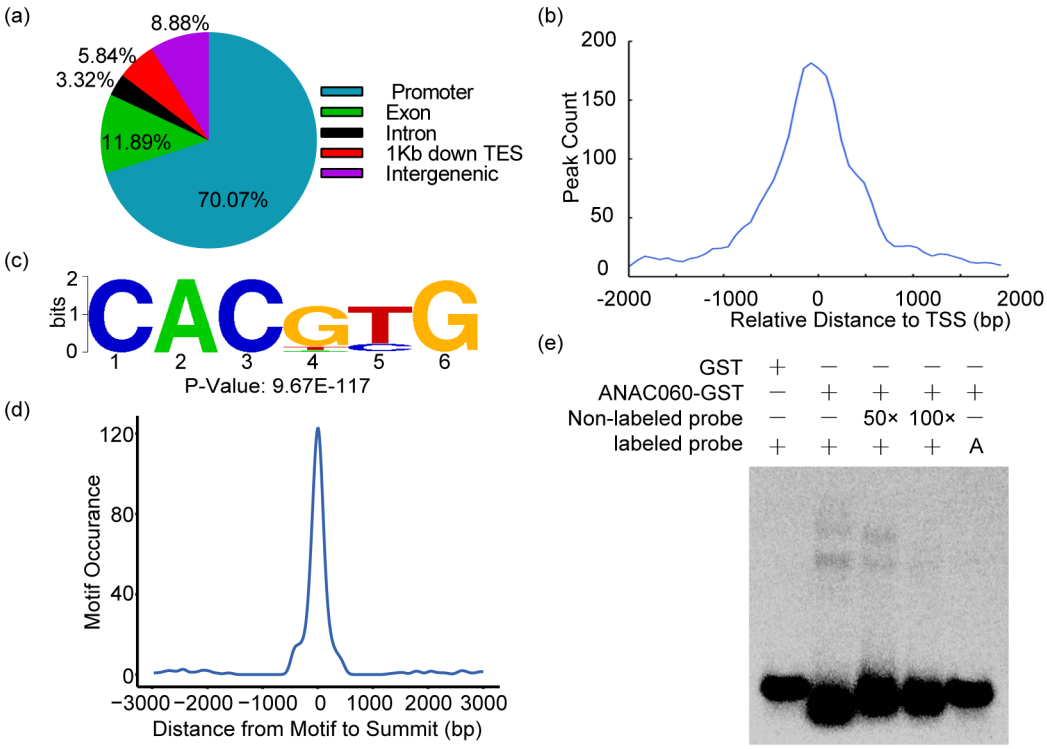

tpj_14777_f2.tif

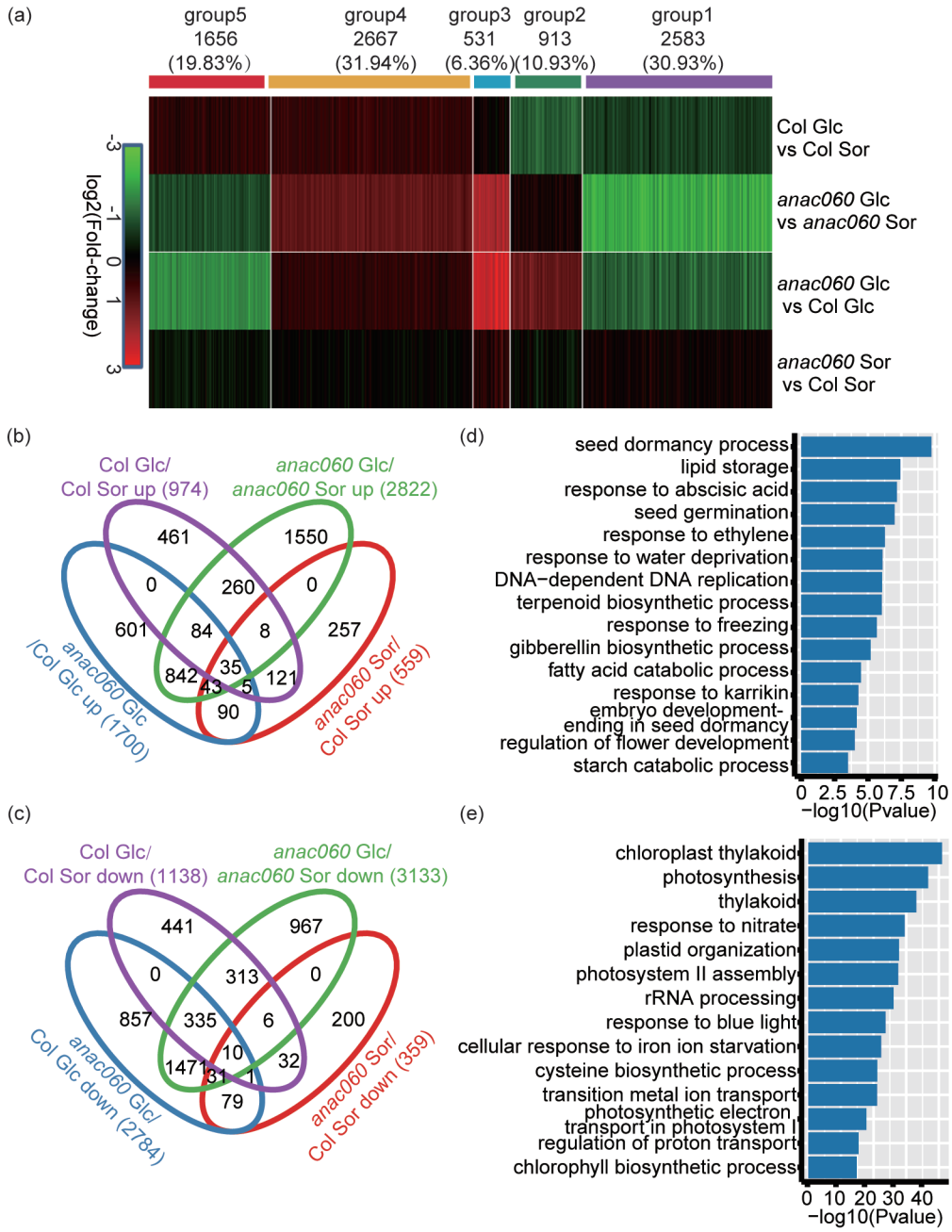

tpj_14777_f3.tif

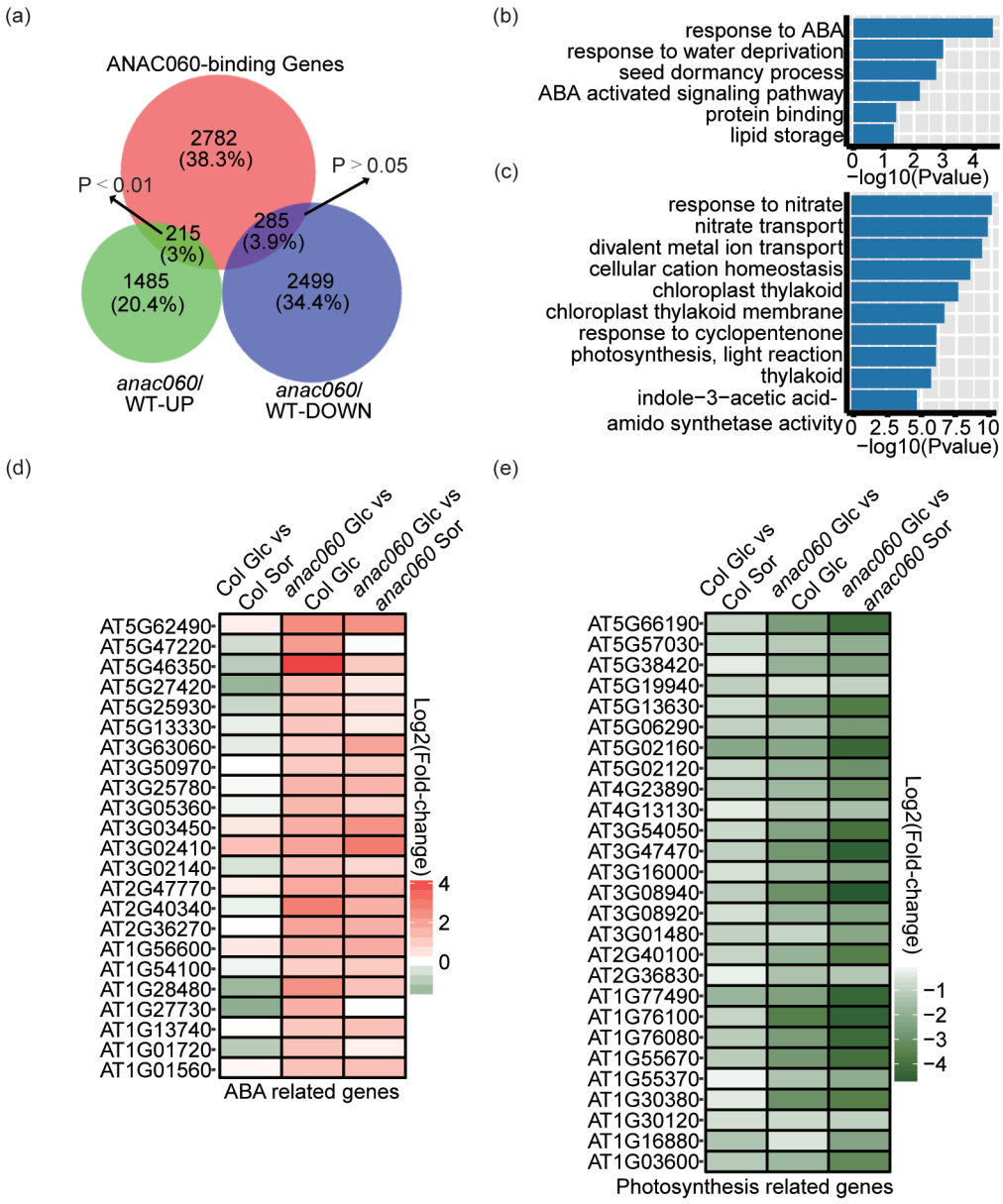

tpj_14777_f4.tif

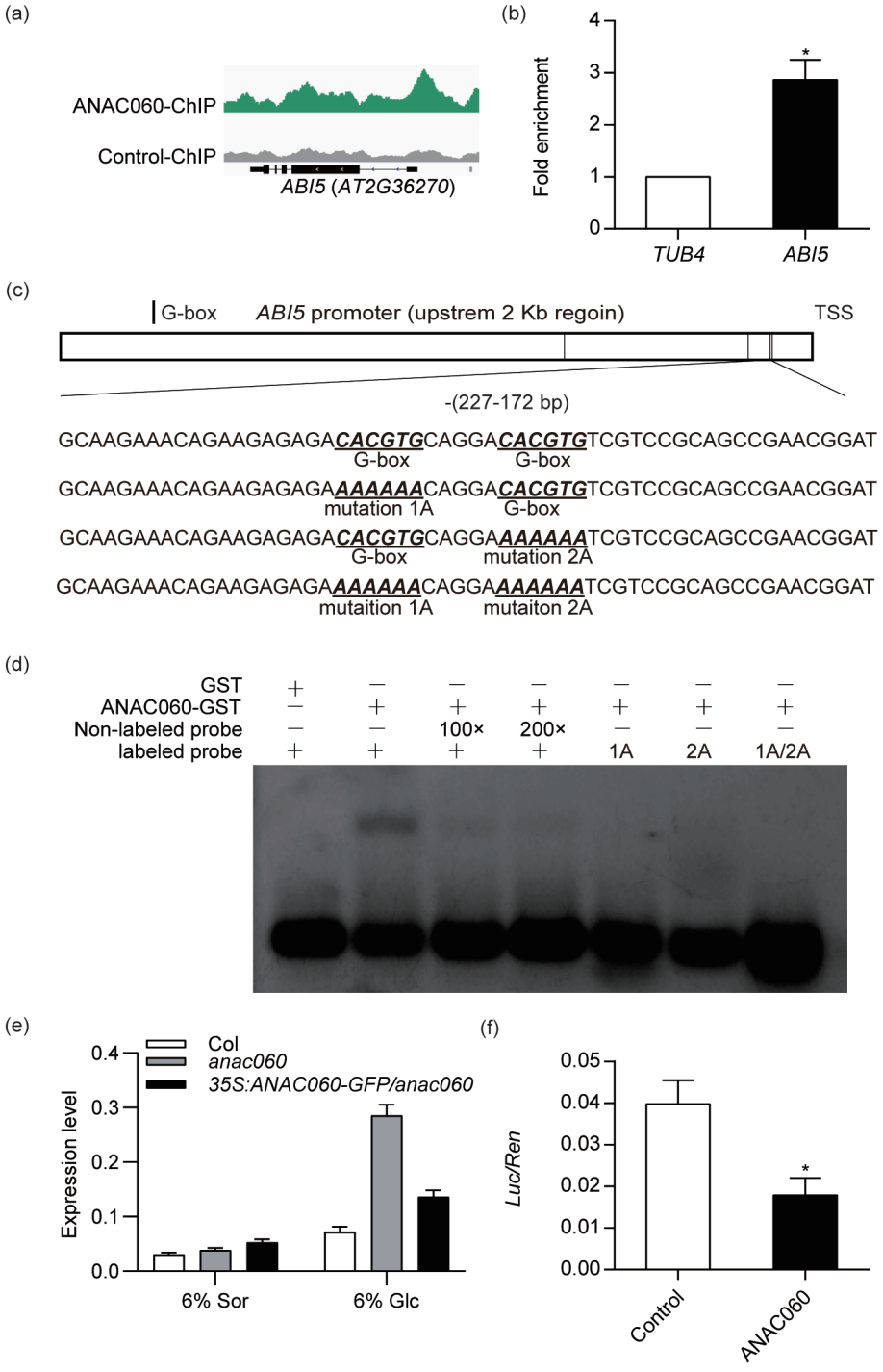

tpj_14777_f5.tif

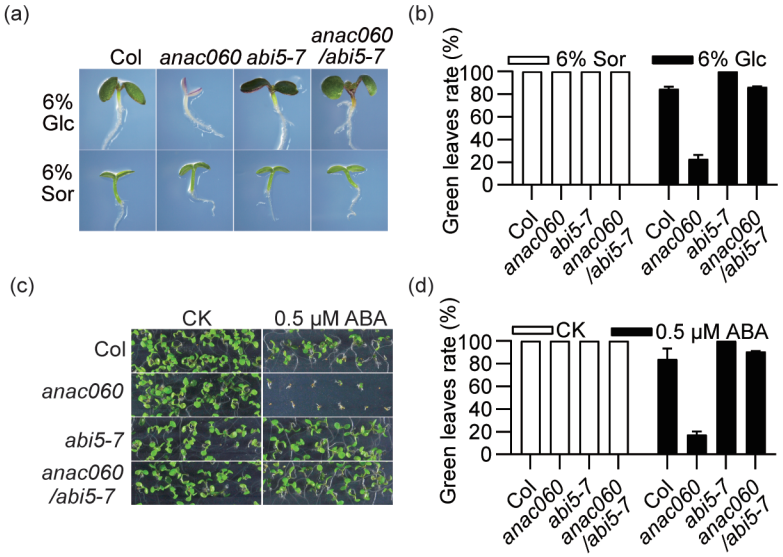

tpj_14777_f6.tif